Spray coated indium-tin-oxide-free organic photodiodes with PEDOT:PSS anodes

Morten Schmidt, Aniello Falco, Marius Loch, Paolo Lugli, and Giuseppe Scarpa

Citation: AIP Advances **4**, 107132 (2014); doi: 10.1063/1.4899044
View online: http://dx.doi.org/10.1063/1.4899044
View Table of Contents: http://scitation.aip.org/content/aip/journal/adva/4/10?ver=pdfcov
Published by the AIP Publishing

Spray coated indium-tin-oxide-free organic photodiodes with PEDOT:PSS anodes

Morten Schmidt,[a] Aniello Falco, Marius Loch, Paolo Lugli,
and Giuseppe Scarpa
Institute for Nanoelectronics, Technical University of Munich, Arcisstr. 21, 80333 Munich, Germany

(Received 25 April 2014; accepted 9 October 2014; published online 17 October 2014)

In this paper we report on Indium Tin Oxide (ITO)-free spray coated organic photodiodes with an active layer consisting of a poly(3-hexylthiophen) (P3HT) and [6,6]-phenyl-C61-butyric acid methyl ester (PCBM) blend and patterned poly(3,4-ethylenedioxythiophene):poly(styrenesulfonate) (PEDOT:PSS) electrodes. External quantum efficiency and current voltage characteristics under illuminated and dark conditions as well as cut-off frequencies for devices with varying active and hole conducting layer thicknesses were measured in order to characterize the fabricated devices. 60% quantum efficiency as well as nearly four orders of magnitude on-off ratios have been achieved. Those values are comparable with standard ITO devices. © *2014 Author(s). All article content, except where otherwise noted, is licensed under a Creative Commons Attribution 3.0 Unported License.* [http://dx.doi.org/10.1063/1.4899044]

I. INTRODUCTION

Organic photovoltaic devices like organic solar cells and organic photodetectors have been attracting a great amount of research.[1,2] They offer promising features as they allow flexible lightweight applications and roll-to roll production of low-cost large area components. However, the indium tin oxide (ITO) commonly used in such devices as transparent electrode material is brittle, thus causing problems in processing flexible devices. Furthermore, the limited availability of indium causes a steady increase of its cost. This has raised the demand for ITO-free devices and alternative transparent electrode materials like graphene,[3] carbon nanotubes,[4] metal nanowire networks[5–8] as well as metal grids[9] and conductive polymers like poly(3,4-ethylenedioxythiophene): poly(styrenesulfonate) (PEDOT:PSS)[10,11] have been investigated.

PEDOT:PSS is a promising candidate as electrode material, due to its easy processabilty, nontoxicity and relatively high conductivity.[11,12] An additional advantage is the possibility to further increase its conductivity by chemical doping.[13] Previous works demonstrated the feasibility of fabricating such ITO free photodiodes[10] and solar cells[14,15] with high conductive PEDOT:PSS as anode and an active layer made of poly(3-hexylthiophen) (P3HT) and [6,6]-phenyl-C61-butyric acid methyl ester (PCBM). However, these devices - produced by means of a lab scale spin-coating technique - show low performance. In case of the photodiodes a high dark current and therefore a low on-off ratio has been reported.[10] The use of spray-technologies[16] would allow one to exploit the high throughput large area production capabilities of this technique which is one of the main advantages of organic electronics, at the same time avoiding the drawbacks of lab scale production processes like spin coating or doctor blading as e.g. the high waste of material. The feasibility of such an approach has been first demonstrated with ITO-free spray coated solar cells.[17] Regarding photodiodes, only devices with an inverted top absorbing structure have been so far demonstrated.[18,19] These devices have been also successfully integrated in organic/inorganic hybrid CMOS-detectors.[20] However, such inverted

[a]Electronic mail: morten.schmidt@nano.ei.tum.de

structures make use of e.g. plasma processes to increase the wettability of the hydrophobic P3HT: PCBM active layer which could negatively affect the device.

In this letter we demonstrate a way to fabricate spray coated ITO-free organic photodiodes with a non inverted structure and patterned PEDOT:PSS anodes as transparent electric contacts. By replacing lithography processes with a shadow mask approach for the patterning of the electrodes, the manufacturing process can be easily transferred to large scale production. A comparative study of standard and ITO-free devices is included.

II. EXPERIMENTAL DETAILS

Devices were fabricated on float glass and prepatterned indium tin oxide coated (ITO) glass samples (Xin Yan Technology Ltd, R_S = 15 Ω/□) which were first sonicated in acetone and isopropanol for 10 minutes. They were subsequently blow dried with nitrogen and treated with oxygen plasma for 1 minute afterwards. In case of non-ITO coated glasses the electrodes where fabricated by heating the sample to 120 °C and spray coating it with a solution consisting of PEDOT:PSS (Clevios PH 1000), deionized water, ethylenglycol (Merck) for increasing the conductivity and the wetting agent Dynol 604 (Sigma-Aldrich) with a weight ratio of 1:1:0.4:0.01 for 60 seconds with a nozzle-to-substrate-distance of 20 cm (see Fig. 1). A shadow mask was used to pattern the film, thus avoiding the use of lithography processes. Afterwards the samples were annealed at 140 °C for 10 minutes to remove any residual moisture in the layer. Subsequently a hole conducting layer (HCL) consisting of PEDOT:PSS (Clevios P VP CH 8000) was spray-deposited. For optimization purposes a series with different layer thicknesses were sprayed. After a second annealing step at 140 °C for 10 minutes a blend consisting of P3HT (Rieke Metals) and PCBM (Solenne B.V.) with a weight ratio of 1:0.75 dissolved in 1,2-dichlorobenzene (Sigma-Aldrich) was sprayed again on top, forming a bulk heterojunction (BHJ), where the layer thickness was varied as well. A last annealing step at 140 °C for 10 minutes in a nitrogen filled glovebox followed. Finally a 100 nm aluminum electrode was deposited by thermal evaporation. All devices were encapsulated using an UV-curing epoxy (Dymax OP4) and a thin glass sheet.

For the reference devices with ITO anode, a previously optimized stack with (HCL:10s, BHJ: 20s (600 nm)) was fabricated using the very same fabrication procedure.

The I-V characterization of the devices was carried out using a Keithley 2602A source meter and a halogen lamp with a light power of 100 mW/cm^2. The external quantum efficiency (EQE) was obtained by using a Newport 74125 Monochromator with a 300 W Xenon arc lamp and a Merlin 70105 Lock-In amplifier. Finally, the cut-off frequency of the devices was evaluated as follows: a Keithley 3390 arbitrary waveform generator produced a square wave voltage with D = 50% duty cycle modulating the optical emission of a green LED (max. 500 μW/cm^2 at 525 nm); the photocurrent of the OPDs was amplified via a FEMTO transconductance amplifier with a gain of 10^4 and the voltage waveforms were analyzed with a LeCroy WavePRO 7zi oscilloscope. The sheet resistance of the PEDOT:PSS anode was measured using a custom-made 4-point prober.

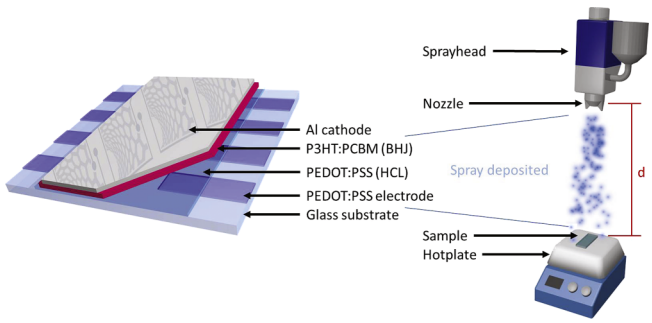

FIG. 1. Schematic of spray setup and a spray coated sample with PEDOT:PSS anode on glass substrate.

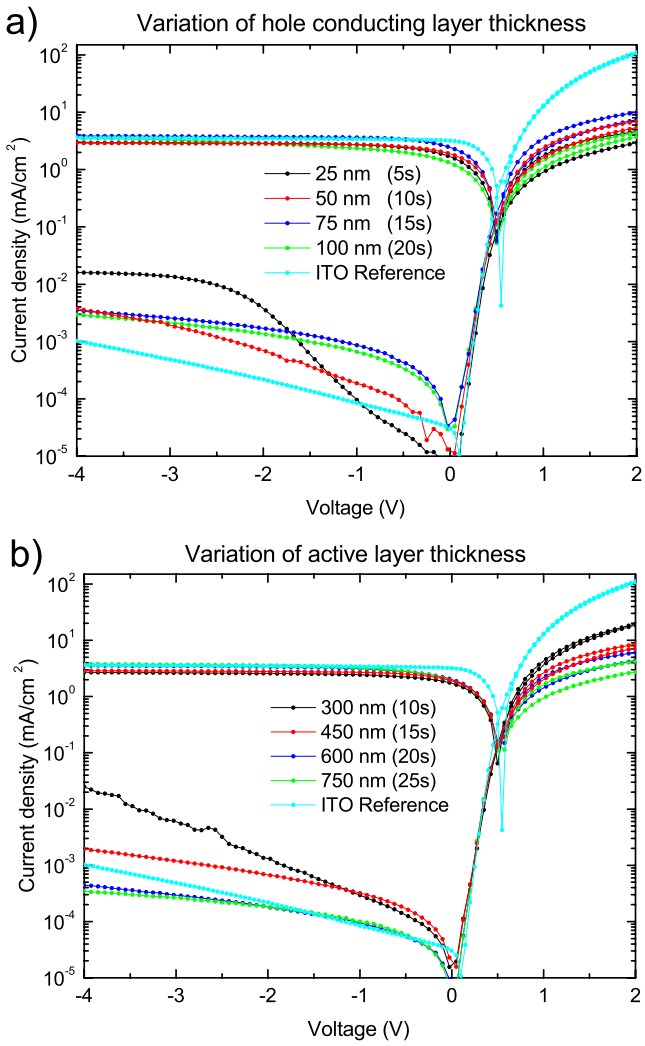

FIG. 2. Logarithmic plot of the I-V-characteristics of samples with a) varying HCL thickness (BHJ thickness for all samples 600 nm) and b) varying BHJ thickness (HCL layer thickness of 50 nm).

III. RESULTS

A. I-V-characteristics

Figure 2 shows the I-V chracteristics of devices fabricated with varying thicknesses of the HCL and BHJ active layer (see supplementary information figures S1 and S2[21]) compared to devices with a BHJ layer thickness of 600 nm and a HCL thickness of 75 nm. The thickness of the HCL (50 nm to 120 nm) is determined by the spray time. In the fact the droplet formation during the spray deposition process results in a layer thickness which can vary strongly. In the case of the BHJ active layer, the thickness can be acquired more accurately as the average layer thickness is much higher (300 nm to 750 nm) and droplet size is significantly smaller due to the different material properties. The I-V characteristics of several samples with increasing HCL thickness are shown in Figure 2(a). They show a strong decrease of the dark current with increasing HCL thickness. The device characteristics for increasing BHJ layer thickness show a similar trend. The photo current of devices with increasing HCL thickness is first increasing and then decreasing. The reduced recombination of electrons diffusing to the anode and the increased roughness are believed to be the reasons for this behavior.[22–26] Once a certain HCL thickness is reached such as all electrons are blocked, the effect will saturate and the photocurrent will decrease, as the serial resistance increases

with HCL thickness as well. This is reflected on the similar behavior shown by the forward current, while the increasing resistance also leads to a decreasing dark current. Compared to a device with ITO electrode the forward current is lower while the photocurrent is basically the same. The reason for this is the lower sheet resistance (R_S) of the ITO electrode of 15 Ω/□ (value given by the manufacturer) compared to the PEDOT:PSS electrode with measured value of ≈100 Ω/□.

Leaving the HCL thickness constant and increasing the BHJ layer thickness (Figure 2(b)) leads to a slight increase in the photocurrent and a drop of the dark current until saturation is reached. A higher proportion of the incident light is absorbed due to the higher absorption of the thicker films. On the other hand, the simultaneously increasing serial resistance is responsible for the decreasing dark current which becomes even lower than that of the ITO reference. This affects in a positive way the performance of the photodetectors, since the on-off ratio of the devices with the thickest BHJ layer are reaching values in the order of nearly 4 orders of magnitude, which is what we measured for the reference diode on ITO. It is worth mentioning that thick active layers, although impacting positively the on-off ratio, hinder a fast operation of the devices (see below).

B. External quantum efficiency

Figure 3 shows the External Quantum Efficiency (EQE) of the fabricated devices, measured at −4 V. Increasing the thickness of the BHJ active layer leads to a reduction in the EQE and to a substantial modification of its shape. In fact, if on the one hand, a thicker BHJ layer guarantees a higher number of collected photons, on the other hand, the probability of recombination is enhanced by the longer average distance from the point in which the charge is generated up to the contacts. The variation in the HCL thickness did not show any clear trend and the differences found are related to process uncertainties. A comparison between the ITO-free fabricated devices and the ITO reference with the optimal HCL/BHJ stack shows an average difference of about 10% in EQE, roughly coincident with the difference in transmittance between the conductive PEDOT:PSS electrode and the ITO. The obtained values of EQE are consistent with the ones found in the literature for ITO-free OPDs.[10]

Another figure of merit of photo detectors is the responsivity of the devices. It can be estimated from the wavelength of the incident light and the quantum efficiency according to the following equation:

$$R = \frac{\eta e \lambda}{hc} \tag{1}$$

The responsivity was found to be between 0.19 A/W and 0.25 A/W at 530 nm for devices with PEDOT:PSS electrode, compared to 0.30 A/W for the ITO reference.

C. Cut-off frequency

The spray-coated diodes on a structured ITO glass gave, on average, cut-off frequencies around 3 kHz (Figure 4) at a light power density of 200 μW/cm^2 at 525 nm (comparable to the sunlight intensity at this wavelength) and were used again as reference to be compared with the fully-spray coated ones.

As shown in the inset of Figure 4, the cut-off frequency is strongly influenced by the overall thickness of the device. Increasing either the BHJ layer or the HCL thickness gives a clear trend of a severe reduction in the cut-off frequency.

Two phenomena seem to be responsible for this behavior. Firstly, as previously stated, to a thicker layer corresponds a longer travel distance for the carriers, meaning that carriers with the same velocity would take, on average, a higher time to get to the contacts. Secondly, since the voltage applied to the electrodes is the same for all devices, the resulting electric field is lower for the thicker ones.

A lower electric field leads to a lower average carrier velocity, hence, at the same time both the velocity is lower and the travel distance is higher: it follows that with an increasing thickness of the layers, the carrier average travel time is increased, with a consequent reduction of the highest

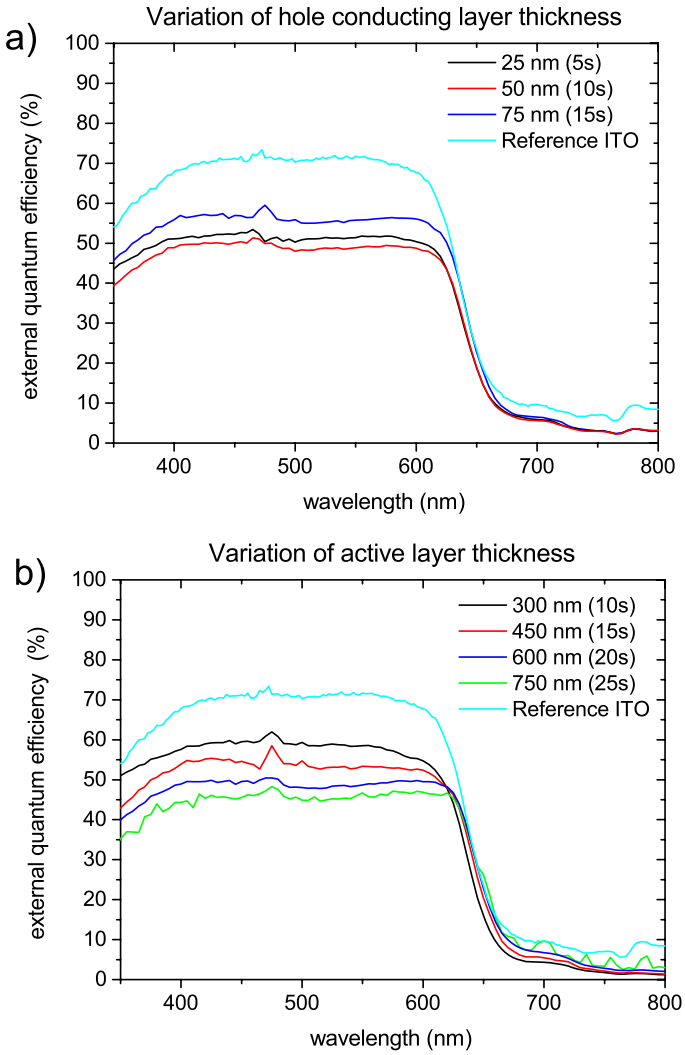

FIG. 3. External quantum efficiency (EQE) measured at −4 V bias voltage of devices with a) varying HCL thickness (BHJ thickness for all samples 600 nm) and b) varying BHJ thickness (HCL thickness 50 nm) both compared to a device (cyan) with ITO anode (HCL:10s (50 nm), BHJ: 20s (600 nm)).

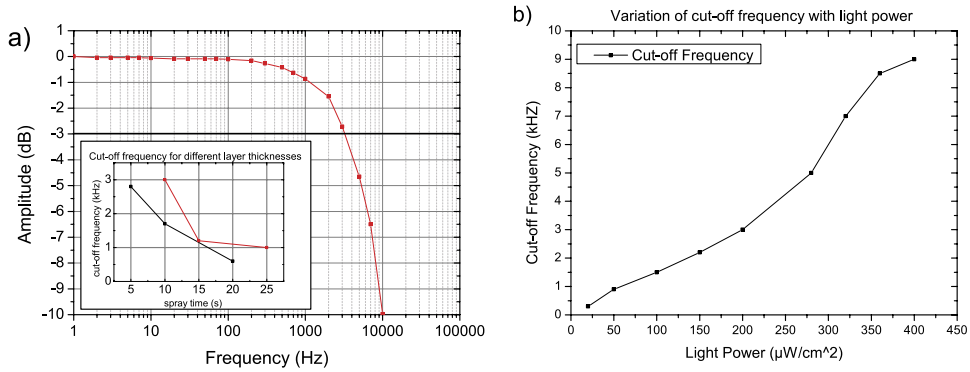

FIG. 4. a) Bode plot of ITO reference device. The inset shows the decrease of cut-off frequency with increasing HCL and BHJ spray time (red BHJ variation, black HCL variation) at 200 $\mu W/cm^2$ light power density. b) Plot cut-off frequency of the best device depending on incident light power density.

TABLE I. Comparisson of ITO free organic photodiodes fabricated with different technologies.

Ref	On-Off ratio (at $-1V$)	EQE (% at 500 nm)	Dark current (mA/cm^2 at $-1V$)	Fabrication technique
Huang *et al.*[10]	≈ 10	50	10^{-3}	Spincoating
Pace *et al.*[27]	≈ 100	32 (−1 V bias)	10^{-3}	Inkjet
Azzellino *et al.*[28]	≈ 10000	65 (−0,9V bias)	10^{-3}	Inkjet
Baierl *et al.*[19]	≈ 100000	70 (−4V bias)	10^{-5}	Spray/inverted
Falco *et al.*[29]	≈ 100000	65 (−5V bias)	10^{-4}	Spray/CNT
This work	≈ 100000	59 (−4V bias)	10^{-4}	Spray

possible operating frequencies. As mentioned above photodiodes optimized in order to achieve a high on-off ratio are limited in their dynamic response, which reduces their field of application to stationary ones.

Figure 4(b) shows how light intensity influences the cut-off frequency for the best performing spray coated diode. A region of quasi-linearity can be noted between 100 $\mu W/cm^2$ and 350 $\mu W/cm^2$, showing a threshold effect for low light intensity and a saturation phenomena for high light intensity.

IV. CONCLUSION

We have demonstrated the fabrication of ITO free P3HT:PCBM-based organic photodiodes using a spray coating manufacturing process. The fabricated devices reach an external quantum efficiency of 62% and on-off-ratios of nearly 4 orders of magnitude. The reached values are comparable to that of ITO free OPDs fabricated with other materials or fabrication techniques as depicted in Table I.

A maximum cut-off frequency of 9 kHz has been reached at a light power of 400 $\mu W/cm^2$. As well as a responsivity of 0.25 A/W at 530 nm. Future work will be devoted to increase the operational frequency of these spray-deposited photodiodes as well as their quantum efficiency.

ACKNOWLEDGMENTS

This work is partially supported by the European Union through FP7-PEOPLE-2012-ITN 316832-OLIMPIA, the TUM Graduate School (TUM-GS), the German Research Foundation (DFG) and the Technical University of Munich within the funding program Open Access Publishing.

[1] J. J. M. Halls, C. A. Walsh, N. Greenham, E. A. Marseglia, R. Friend, S. C. Moratti, and A. Holmes, "Efficient photodiodes from interpenetrating polymer networks," Nature **376**, 498–500 (1995).
[2] G. Yu, J. Gao, J. C. Hummelen, F. Wudl, and A. J. Heeger, "Polymer photovoltaic cells: Enhanced efficiencies via a network of internal donor-acceptor heterojunctions," Science **270**, 1789–1791 (1995).
[3] M. P. Ramuz, M. Vosgueritchian, P. Wei, C. Wang, Y. Gao, Y. Wu, Y. Chen, and Z. Bao, "Evaluation of solution-processable carbon-based electrodes for all-carbon solar cells," ACS Nano **6**, 10384–10395 (2012).
[4] M. W. Rowell, M. A. Topinka, M. D. McGehee, H.-J. Prall, G. Dennler, N. S. Sariciftci, L. Hu, and G. Gruner, "Organic solar cells with carbon nanotube network electrodes," Applied Physics Letters **88**, 233506 (2006).
[5] S. De, T. M. Higgins, P. E. Lyons, E. M. Doherty, P. N. Nirmalraj, W. J. Blau, J. J. Boland, and J. N. Coleman, "Silver nanowire networks as flexible, transparent, conducting films: Extremely high dc to optical conductivity ratios," ACS Nano **3**, 1767–1774 (2009).
[6] J. van de Groep, P. Spinelli, and A. Polman, "Transparent conducting silver nanowire networks," Nano Letters **12**, 3138–3144 (2012).
[7] H. Wu, D. Kong, Z. Ruan, P.-C. Hsu, S. Wang, Z. Yu, T. J. Carney, L. Hu, S. Fan, and Y. Cui, "A transparent electrode based on a metal nanotrough network," Nature Nanotechnology (2013).
[8] D.-S. Leem, A. Edwards, M. Faist, J. Nelson, D. D. C. Bradley, and J. C. de Mello, "Efficient organic solar cells with solution-processed silver nanowire electrodes," Adv. Mater. **23**, 4371–4375 (2011).
[9] J. Zou, H.-L. Yip, S. K. Hau, and A. K.-Y. Jen, "Metal grid/conducting polymer hybrid transparent electrode for inverted polymer solar cells," Applied Physics Letters **96**, 203301 (2010).
[10] J. Huang, X. Wang, Y. Kim, A. J. deMello, D. D. C. Bradley, and J. C. deMello, "High efficiency flexible ito-free polymer/fullerene photodiodes," Physical Chemistry Chemical Physics **8**, 3904–3908 (2006).

[11] H. Do, M. Reinhard, H. Vogeler, A. Puetz, M. F. Klein, W. Schabel, A. Colsmann, and U. Lemmer, "Polymeric anodes from poly(3,4-ethylenedioxythiophene):poly(styrenesulfonate) for 3.5% efficient organic solar cells," Thin Solid Films **517**, 5900–5902 (2009).
[12] Y. Zhou, F. Zhang, K. Tvingstedt, S. Barrau, F. Li, W. Tian, and O. Inganas, "Investigation on polymer anode design for flexible polymer solar cells," Applied Physics Letters **92**, 233308 (2008).
[13] Y. H. Kim, C. Sachse, M. L. Machala, C. May, L. Müller-Meskamp, and K. Leo, "Highly conductive pedot:pss electrode with optimized solvent and thermal post-treatment for ito-free organic solar cells," Advanced Functional Materials **21**, 1076–1081 (2011).
[14] S.-I. Na, S.-S. Kim, J. Jo, and D.-Y. Kim, "Efficient and flexible ito-free organic solar cells using highly conductive polymer anodes," Advanced Materials **20**, 4061–4067 (2008).
[15] Y.-S. Hsiao, W.-T. Whang, C.-P. Chen, and Y.-C. Chen, "High-conductivity poly(3,4-ethylenedioxythiophene):poly(styrene sulfonate) film for use in ito-free polymer solar cells," J. Mater. Chem. **18**, 5948–5955 (2008).
[16] A. Abdellah, K. S. Virdi, R. Meier, M. Döblinger, P. Müller-Buschbaum, C. Scheu, P. Lugli, and G. Scarpa, "Successive spray deposition of p3ht/pcbm organic photoactive layers: Material composition and device characteristics," Adv. Funct. Mater. **22**, 4078–4086 (2012).
[17] S.-I. Na, B.-K. Yu, S.-S. Kim, D. Vak, T.-S. Kim, J.-S. Yeo, and D.-Y. Kim, "Fully spray-coated ito-free organic solar cells for low-cost power generation," Solar Energy Materials and Solar Cells **94**, 1333–1337 (2010).
[18] D. Baierl, B. Fabel, P. Gabos, L. Pancheri, P. Lugli, and G. Scarpa, "Solution-processable inverted organic photodetectors using oxygen plasma treatment," Organic Electronics **11**, 1199–1206 (2010).
[19] D. Baierl, B. Fabel, P. Lugli, and G. Scarpa, "Efficient indium-tin-oxide (ito) free top-absorbing organic photodetector with highly transparent polymer top electrode," Organic Electronics **12**, 1669–1673 (2011).
[20] D. Baierl, L. Pancheri, M. Schmidt, D. Stoppa, G.-F. Dalla Betta, G. Scarpa, and P. Lugli, "A hybrid cmos-imager with a solution-processable polymer as photoactive layer," Nature Communications **3**, 1175 (2012).
[21] See supplementary material at http://dx.doi.org/10.1063/1.4899044 for details on thickness measurements of the active layers and sheet resistance of PEDOT:PSS layers.
[22] R. Po, C. Carbonera, A. Bernardi, and N. Camaioni, "The role of buffer layers in polymer solar cells," Energy Environ. Sci. **4**, 285–310 (2011).
[23] H. Ma, H.-L. Yip, F. Huang, and A. K.-Y. Jen, "Interface engineering for organic electronics," Advanced Functional Materials **20**, 1371–1388 (2010).
[24] C. Deibel and V. Dyakonov, "Polymer-fullerene bulk heterojunction solar cells," Reports on Progress in Physics **73**, 096401 (2010).
[25] A. Elschner, S. Kirchmeyer, W. Lovenich, U. Merker, and K. Reuter, *PEDOT: Principles and Applications of an Intrinsically Conductive Polymer* (CRC Press, 2010), p. 147.
[26] B. Friedel, P. E. Keivanidis, T. J. K. Brenner, A. Abrusci, C. R. McNeill, R. H. Friend, and N. C. Greenham, "Effects of layer thickness and annealing of pedot:pss layers in organic photodetectors," Macromolecules **42**, 6741–6747 (2009).
[27] G. Pace, A. Grimoldi, D. Natali, M. Sampietro, J. E. Coughlin, G. C. Bazan, and M. Caironi, "All-organic and fully-printed semitransparent photodetectors based on narrow bandgap conjugated molecules," Advanced Materials (2014).
[28] G. Azzellino, A. Grimoldi, M. Binda, M. Caironi, D. Natali, and M. Sampietro, "Fully inkjet-printed organic photodetectors with high quantum yield," Advanced Materials **25**, 6829–6833 (2013).
[29] A. Falco, L. Cinà, G. Scarpa, P. Lugli, and A. Abdellah, "Fully-sprayed and flexible organic photodiodes with transparent carbon nanotube electrodes," ACS Applied Materials & Interfaces **6**, 10593–10601 (2014).